

Jeongin Lee¹ and Tae-Kyung Hong^{1*}

⁶ ¹Yonsei University, Department of Earth System Sciences, 50 Yonsei-ro, Seodaemun-gu
⁷ Seoul 03722, South Korea.

¹⁰ tkhong@yonsei.ac.kr (Tae-Kyung Hong)



Abstract

The COVID-19 virus has a high infection rate, spreading fast in the world. Lockdown and stay-at-home actions have been taken in many countries to reduce the rate of the virus spreading. The daytime ambient seismic noises in 11 major cities of 7 countries are assessed. Daytime seismic noises in 10 am to 6 pm at frequencies ≥ 2 Hz are assessed. The seismic noise levels are compared with the community mobility data that represent the human activities. The high-frequency seismic noise levels present high correlation with the human activities. The human activities decrease with the number of daily confirmed cases. The peak noise-level reductions in lockdown periods were as high as 42-96 %. The noise levels generally started to decrease since the days when the daily confirmed cases reached ~ 500 . The noise level variation presents the lockdown progress. The noise level recovers with time since the end of lockdown. The high correlation between seismic noise level and community mobility suggests possible utilization of seismic noises for anonymous monitoring of human activities.



1 Introduction

COVID-19 spreads fast in the world. The high infectivity of the virus changes human life. The World Health Organization (WHO) recommended social distancing to slow down the spreading rate. Social distancing and wearing a mask may be the only ways to reduce the infection rate. Many countries locked down cities and shutdown workplaces to block the spread of the virus. However, the effectivity and effective maintenance period of social distancing is unknown. Further, it is difficult to assess the level of social activity of people.

Fluid population is crucial information to be collected. Realtime mobility data may be useful to identify the fluid population at certain locations. Location-based information is necessary to account the level of lockdowns. Big data from location-based service (LBS) for mobile internet can be applied in this regard. However, the information from location-based service may suffer from privacy infringement that is a critical issue in data acquisition. Further, publicly open big data is limited available.

Ambient seismic noise represents ground responses to a composite effect of microseismic sources that include anthropogenic (cultural) sources such as traffic, construction, cultural activity, and industrial operations (Groos and Ritter, 2009; Larose et al., 2015; Riahi and Gerstoft, 2015; Coward et al., 2003; Fuchs et al., 2018). Human activity is a major source of ambient seismic noises greater than 2 Hz (Plesinger and Wielandt, 1974; Kar and Mohanty, 2006; Bokelmann and Baisch, 2008; Hong et al., 2020). Human activities produce high-frequency ground vibrations that decay fast with distance (Aki and Wu, 1988; Hong et al., 2005; Diaz, 2016). High-frequency ambient seismic noise field develops by scattering in the crust (Aki and Wu, 1988; Sato and Fehler, 1997; Hong and Kennett, 2003, 2004; Hong et al., 2004).

High-frequency ambient seismic noises may represent the level of human activities (Groos and Ritter, 2009; Hong et al., 2020). Recently, it was reported that high-frequency seismic-noise levels are correlated with economic growth (Hong et al., 2020). The noise levels may be used for realtime monitoring of economic condition. Thus, seismic noises may be useful to treat the personal identity anonymously for assessment of human activities.

The lockdowns in COVID-19 pandemic provide a chance to examine the correlation between seismic noise level and human activity level (Lecocq et al., 2020; Denolle and



56 Nissen-Meyer, 2020; Dias et al., 2020). We examine the utility of seismic noises as a tool
 57 to assess the human activities without privacy infringement.

58 2 Data and COVID-19

59 The first confirmed case of COVID-19 virus infection was reported in Wuhan, China on
 60 December 31, 2019. We analyze the ambient seismic noise levels before and after the
 61 virus outbreak and social distancing (Gibney, 2020). We consider 7 representative countries
 62 including China, South Korea, France, Spain, Italy, the UK, and the USA. China and South
 63 Korea had the first and second largest numbers of confirmed cases by March 9, 2020,
 64 respectively. China and South Korea experienced high contagion followed by a recession
 65 in the infection rate. The contagion cases were concentrated in local regions: Daegu and
 66 Gyeongsangbuk-do Province in South Korea and Wuhan and Hubei Province in China. France,
 67 Spain, Italy, the UK, and the USA experienced fast spreading after China and South Korea.
 68 Further, the countries are distributed in Asia, Europe, and North America of the northern
 69 hemisphere that may have comparable seasonal effects in virus spreading (Fig. 1).

70 Enshi in Hubei Province, China was locked down on January 24. Hubei Province was
 71 released from lockdown on March 25. The first confirmed case in South Korea occurred on
 72 January 20 (Fig. 1). The number of confirmed cases increased rapidly following the mass
 73 contagion in Sincheonji Church, Daegu, on February 18. Daegu experienced a high increase in
 74 confirmed cases after February 21. The confirmed cases in South Korea are concentrated in
 75 Daegu and Gyeongsangbuk-do Province. Stay-at-home action was taken in Daegu on February
 76 20. High-intensity social distancing setting has been in effect since March 23 in South Korea.

77 Many countries enacted lockdowns or equivalent governmental actions to reduce outdoor
 78 activities. Italy, France, and the UK went into lockdown on March 10 (northern Italy on March
 79 9), March 17, and March 23, respectively. Spain and New York in the USA declared a state of
 80 national emergency on March 15 and March 20, respectively. We collect the information on the
 81 global confirmed cases from from the World Health Organization (<https://covid19.who.int/>)
 82 and Korea Centers for Disease Control & Prevention (<http://ncov.mohw.go.kr/en/>). The
 83 numbers of confirmed cases generally decrease after lockdowns with time delays (Fig. 1).
 84 China and South Korea present rapid decay in the numbers of daily confirmed cases. Italy,



85 France, and Spain present mild decreases in the numbers of daily confirmed cases, while USA
 86 and UK display slow decays (Fig. 1).

87 We select 11 cities of the seven countries where high rates of virus infection were reported in
 88 the early pandemic. The cities are Paris (France), Marseilles (France), Madrid (Spain), Milan
 89 (Italy), Rome (Italy), Edinburgh (UK), New York (USA), Los Angeles (USA), Seoul (South
 90 Korea), Enshi (Hubei Province, China), and Beijing (China). We collect continuous vertical
 91 records of broadband or short-period seismic stations in the cities in 7 countries where high
 92 infection rates have occurred (Fig. 1). The seismic records are collected from the Incorporated
 93 Research Institutions for Seismology and the Korea Meteorological Administration. The
 94 sampling rates are 40, 50 or 100 Hz. The analyzed periods are December 2019 to May 2020 for
 95 the cities in China (Enshi and Beijing) and February 2020 to May 2020 for the other cities.

96 Community mobility data provide information of human activities in local regions. We
 97 collect the human mobility data from Google (<https://www.google.com/covid19/mobility/>).
 98 The Google mobility data is available since mid-February, 2020. The mobility data for grocery
 99 and pharmacy business decrease mildly since the pandemic, recovering faster than other
 100 business types. The mobility data for retail and recreation business, workplace, and transit
 101 stations vary similarly one another.

102 3 Seismic noise analysis

103 We examine the spectra of continuous vertical velocity records (Fig. 2). Spectral composition
 104 of seismic noises is site-dependent. Anthropogenic noises are primary components in ambient
 105 seismic-noise field in frequencies ≥ 2 Hz (Coward et al., 2003; Fuchs et al., 2018; Hong et al.,
 106 2020). The vertical velocity spectra present weak ambient noises at frequencies $\geq \sim 2$ Hz since
 107 the virus outbreak and social distancing (Fig. 2). The weakening of ambient noise is observed
 108 in wide high frequency ranges. The noise weakening recovers since lockdown release.

109 Considering the spectral contents of seismic noises, we choose frequency bands of 5-15
 110 Hz for analysis (Fig. 3). We analyze seismic records at frequencies 2-4 Hz for stations with
 111 incidental high-frequency noises (stations BJT and ENH) (Fig. 3). Seismic noises from the
 112 other stations are analyzed in frequencies of 5-15 Hz. We calculate the power spectral density



(PSD) based on 2-hour time windows that are shifted by 1 hour with 50 % overlap (Fig. 4).
 The seismic noise levels present daily periodicity and diurnal variations.

The diurnal variation in high-frequency noise levels resembles the diurnal cycle of human activities. Daytime noise levels are higher than nighttime noise levels (Groos and Ritter, 2009; Diaz, 2016) (Fig. 5). The noise levels on weekdays are stronger than those on weekends and holidays. The seismic noise levels decrease temporarily in lunch time.

We assess the daytime ambient seismic noises at 10 am to 6 pm to represent the daily noise levels (Fig. 6). The seismic noise levels are high in daytime and low in nighttime. We determine the representative noise levels by stacking the daytime PSDs (Fig. 7). The daily noise levels present weekly periodicity. We use only the weekday noise levels excluding the noise levels in weekends. The noise levels present apparent noise decrease during weekends (Fig. 8). An analysis of weekday noise level may enable us to assess the level of social and economic activities (Hong et al., 2020).

4 Ambient noise level variation

We observe fast decay in seismic noise levels after January 14. The ambient noise levels in Enshi and Beijing decreased rapidly before the city lockdown (Fig. 9). The low noise level in Enshi continued until mid-March and started to increase before the city release on March 25. On the other hand, the noise level in Beijing started to increase gradually in early February, and recovered fully in mid-April.

The seismic stations in Beijing and Enshi, China present low seismic noises in late January to March. The ambient seismic noises in frequencies greater than 2 Hz display similar feature (Fig. 9). The daytime noise levels in Seoul decreased mildly between January 30 and March 9, after which it gradually recovered (Fig. 9).

The noise levels in Rome and Milan, Italy, decreased after March 9. Similar features have been observed in Madrid since March 9, Edinburgh since March 16, New York and Los Angeles since March 12, and Paris and Marseilles since March 17. It is intriguing to note that the noise levels in most regions started to decrease even before the lockdown or equivalent governmental actions were enacted. This observation suggests that people might have concern about the



141 fast spreading of the virus in the regions, reducing their outdoor activities spontaneously. The
142 noise level decreased further after governmental actions.

143 The noise levels dropped by 42-96 % relative to the usual daily noise levels on weekdays in
144 the countries that experienced lockdown or equivalent governmental actions (Fig. 9). The noise
145 level in Seoul decreased only by 9 %, recovering gradually with decreasing daily confirmed
146 cases in South Korea.

147 5 Correlation with mass mobility data

148 We compare the daily noise level changes with the human mobility volume changes of various
149 business (Fig. 9). The human mobility decreases as telecommuting and shutdown of workplaces
150 increase. The seismic noise levels present correlations with the mobility data. The levels of
151 correlations between the ambient noises and mobility data are different by business type.
152 Also, the magnitude of noise-level decrease is different by region. This may be partly because
153 the medium responses to the human activities and composition of human activities and
154 populations are different by region.

155 The high correlation between noise level and human mobility suggests that the
156 high-frequency seismic noises are mainly excited by human activities (Groos and Ritter, 2009;
157 Larose et al., 2015; Hong et al., 2020; Gibney, 2020). The decreasing seismic noises suggest
158 decreasing ground-motion inducing sources. The seismic noise levels and human activities
159 decrease with the number of daily confirmed cases (Fig. 10). The correlation suggests that
160 both the noise level and mobility data may represent the human activities reasonably. The
161 seismic noises may be useful for monitoring of human activity, keeping anonymity.

162 6 Discussion and conclusions

163 The noise-level decrease suggests effective social distancing. The daily confirmed cases started
164 to decrease in 11-32 days after the effective social distancing (gray boxes in Fig. 10). This
165 observation suggests that social distancing may be an effective way to reduce the infection
166 rate. It is noteworthy that the daily confirmed cases increased continuously for some times
167 (i.e., 11-32 days) after the effective social distancing. The observation suggests that the social



168 distancing has the reserve time of two weeks to one month to be effective for reducing the
169 daily confirmed cases.

170 The number of cumulative confirmed cases appears to be correlated with the time lapsed
171 until the effective social distancing. However, the lapse time is different by country; the
172 noise-level decrease (i.e., effective social distancing) took place mostly around the first date
173 of 500 or more daily confirmed cases in the country (UK, USA, France, Spain, and Italy).

174 The noise-level decay rate may represent the level of public participation (lapse times in
175 red boxes in Fig. 10). A large decay rate of noise level may suggest high public participation.
176 The effectivity of social distancing may be dependent on the level of social distancing and
177 public participation. This observation suggests that confirmed cases may start to decrease
178 sooner if social distancing is enacted earlier.

179 The high-frequency seismic noise levels are reasonably represented by mobility data. The
180 relative influence of human activities on seismic noises is different by city. It is noteworthy
181 that human mobility data is limitedly available due to the privacy infringement. The high
182 correlation with mobility data suggests that the ambient noise may be used for realtime
183 monitoring for the human mobility without privacy infringement. This observation suggests
184 that the seismic noise data may replace the big data information.

185 Data availability

186 The data and results of this study will be available on Dryad (<https://datadryad.org/stash>)
187 when the paper is published.

188 Author contributions

189 JL collected data, performed analyses, and prepared figures. TKH led the research, guided
190 the analyses, developed the methods, and wrote the manuscript. JL and TKH discussed the
191 results.



192 Competing interests

193 The authors declare that they have no conflict of interest.

194 Acknowledgments

195 The seismic data were collected from the Incorporated Research Institutions for
 196 Seismology (IRIS, <https://www.iris.edu>) and the Korea Meteorological Administration
 197 (KMA, <https://www.weather.go.kr>).

198 Financial support

199 This work was supported by the Korea Meteorological Administration Research and
 200 Development Program under grant KMI2018-02910. Additionally, this research was partly
 201 supported by National Research Foundation of Korea (NRF-2017R1A6A1A07015374,
 202 NRF-2018R1D1A1A09083446).

203 References

- 204 Aki, K., and R.-S. Wu (1988), Scattering and Attenuations of Seismic Waves, Part 1,
 205 Springer, Basel, p446.
- 206 Bokelmann, G. H. R., and S. Baisch (1999), Nature of narrow-Band signals at 2.083 Hz,
 207 Bulletin of the Seismological Society of America, 89 (1), 156-164.
- 208 Coward, D., D. Blair, R. Burman, and C. Zhao (2003), Vehicle-induced seismic effects at a
 209 gravitational wave observatory, Review of Scientific Instruments, 74 (11), 4846-4854.
- 210 Denolle, M.A., and T. Nissen-Meyer (2020), Quiet Anthropocene, quiet Earth, Science, 369
 211 (6509), 1299-1300.
- 212 Dias, F.L., M. Assumpção, P.S. Peixoto, M.B. Bianchi, B. Collaco, J. Calhau (2020),
 213 Using Seismic Noise Levels to Monitor Social Isolation: An Example From Rio de
 214 Janeiro, Brazil, Geophysical Research Letters, 47, e2020GL088748. <https://doi.org/10.1029/2020GL088748>.
- 215
 216 Díaz, J. (2016), On the origin of the signals observed across the seismic spectrum,
 217 Earth-Science Reviews, 161, 224-232.



- 218 Fuchs, F., G. Bokelmann, and the AlpArray Working Group (2018), Equidistant spectral
 219 lines in train vibrations, *Seismological Research Letters*, 89 (1), 56-66.
- 220 Gibney, E. (2020), Coronavirus lockdowns have changed the way Earth moves, *Nature*, 580,
 221 1706-177.
- 222 Groos, J. C., and J. R. R. Ritter (2009), Time domain classification and quantification
 223 of seismic noise in an urban environment, *Geophysical Journal International*, 179 (2),
 224 1213-1231.
- 225 Hong, T.-K. and B.L.N. Kennett (2003), Scattering attenuation of 2D elastic waves: theory
 226 and numerical modeling using a wavelet-based method, *Bulletin of the Seismological Society*
 227 *of America*, 93 (2), 922-938.
- 228 Hong, T.-K. and B.L.N. Kennett (2004), Scattering of elastic waves in media with a random
 229 distribution of fluid-filled cavities: theory and numerical modelling, *Geophysical Journal*
 230 *International*, 159 (3), 961-977.
- 231 Hong, T.-K., B.L.N. Kennett, and R.-S. Wu (2004), Effects of the density perturbation in
 232 scattering, *Geophysical Research Letters*, 31 (13), L13602, doi:10.1029/2004GL019933.
- 233 Hong, T.-K., J. Lee, G. Lee, J. Lee, and S. Park (2020), Correlation between ambient seismic
 234 noises and economic growth, *Seismological Research Letters*, *Seismological Research Letters*,
 235 91 (4), 2343-2354.
- 236 Hong, T.-K., R.-S. Wu, and B.L.N. Kennett (2005), Stochastic features of scattering, *Physics*
 237 *of the Earth and Planetary Interiors*, 148 (2-4), 131-148.
- 238 Kar, C., and A. R. Mohanty (2006), Monitoring gear vibrations through motor current
 239 signature analysis and wavelet transform, *Mechanical Systems and Signal Processing*, 20
 240 (1), 158-187.
- 241 Larose, E., S. Carriere, C. Voisin, P. Bottelin, L. Baillet, P. Gueguen, F. Walter, D. Jongmans,
 242 B. Guillier, S. Garambois, F. Gimbert, and C. Massey (2015), Environmental seismology:
 243 What can we learn on earth surface processes with ambient noise?, *Journal of Applied*
 244 *Geophysics*, 116, 62-74.
- 245 Lecocq, T., S.P. Hicks, K. Van Noten, K. van Wijk, P. Koelemeijer, R. S. M. De Plaen, F.
 246 Massin, G. Hillers, R. E. Anthony, M.-T. Apoloner, M. Arroyo-Solorzano, J.D. Assink, P.
 247 Büyükkakpınar, A. Cannata, F. Cannavo, S. Carrasco1, C. Caudron, E. J. Chaves, D. G.



- 248 Cornwell, D. Craig, O. F. C. den Ouden, J. Diaz, S. Donner, C. P. Evangelidis, L. Evers,
249 B. Fauville, G. A. Fernandez, et al. (2020), Global quieting of high-frequency seismic noise
250 due to COVID-19 pandemic lockdown measures, *Science*, 369, 1338-1343.
- 251 Plesinger, A., and E. Wielandt (1974), Seismic noise at 2 Hz in Europe, *Journal of Geophysics*,
252 40, 131-136.
- 253 Riahi, N., and P. Gerstoft (2015), The seismic traffic footprint: Tracking trains, aircraft, and
254 cars seismically, *Geophysical Research Letters*, 42, 2674-2681.
- 255 Sato, H., and M.C. Fehler (1997), *Seismic Wave Propagation and Scattering in the*
256 *Heterogeneous Earth*, Springer, Berlin, p304.



Figure 1. (a) Map of 11 seismic stations in 7 countries and temporal variations of confirmed cases for (b) China, (c) Italy, (d) France, (e) United States of America, (f) United Kingdom, (g) Spain, and (h) South Korea. Continuous vertical seismic records are collected from the seismic stations. The daily and cumulative numbers of confirmed cases are presented. The lockdown starting dates and released dates are marked.

Figure 2. Temporal variation of spectral amplitudes: (a) map of stations and periods, and vertical spectrograms for stations (b) BJT, (c) ARBF, and (d) RMP. The lockdown starting dates and released dates are indicated. The first dates of 10, 50, 100, 500 daily confirmed cases are marked. The seismic noises decrease apparently during the lockdown periods.

Figure 3. Spectral contents of ambient seismic noises before the COVID-19 outbreak at stations (a) RMP in Rome and (b) ENH in Enshi. Ambient seismic noises in frequencies ≥ 2 Hz present daily periodicity and diurnal variations associated with human activities. Frequency bands of 5-15 Hz or 2-4 Hz are used for seismic noise analysis.

Figure 4. Vertical power spectral density (PSD) variation at frequencies of 5-15 Hz or 2-4 Hz in stations (a) BJT in Beijing, (b) ENH in Enshi, (c) RMP in Rome, (d) MILN in Milan, (e) ARBF in Marseilles, (f) S1108 in Paris, (g) CPNY in New York, (h) USC in Los Angeles, (i) EDI in Edinburgh, (j) UCM in Madrid, and (k) SEO in Seoul. Power spectral densities of seismic noises are presented. The cumulative numbers of confirmed cases are presented. The noise levels are low in March and April in most stations.

Figure 5. Vertical power spectral densities in frequencies of 5-15 Hz at stations (a) RMP in Rome and (b) CPNY in New York in February 2020 before the virus outbreak in Italy. Weekends (Saturdays, Sundays) are marked. The seismic-noise amplitudes are large in weekdays, and small in weekends.

Figure 6. Diurnal variation of seismic noise amplitudes in weekdays at stations (a) RMP in Rome and (b) CPNY in New York. The analyzed daytime seismic noises are marked. The daytime noise levels are larger than the nighttime noise levels. The seismic noises are weak in lunchtime.



Figure 7. Daily average seismic noise levels at frequencies at frequencies of 5-15 Hz or 2-4 Hz in stations (a) BJT in Beijing, (b) ENH in Enshi, (c) RMP in Rome, (d) MILN in Milan, (e) ARBF in Marseilles, (f) S1108 in Paris, (g) CPNY in New York, (h) USC in Los Angeles, (i) EDI in Edinburgh, (j) UCM in Madrid, and (k) SEO in Seoul. Power spectral densities of seismic noises are presented. The cumulative numbers of confirmed cases are presented.

Figure 8. Representative daily seismic noise variation at stations (a) RMP in Rome and (b) CPNY in New York. The noise levels in weekends are excluded to avoid the weekend effect. The noise levels in weekends are presented for comparison.

Figure 9. Comparison between seismic noise level changes and mobility data at stations (a) RMP in Rome, (b) MILN in Milan, (c) ARBF in Marseilles, (d) S1108 in Paris, (e) CPNY in New York, (f) USC in Los Angeles, (g) EDI in Edinburgh, (h) UCM, Madrid, and (g) SEO in Seoul. The daily numbers of confirmed cases are presented.

Figure 10. Ambient noise-level changes and daily confirmed cases in 7 countries (UK, USA, France, Spain, Italy, South Korea, and China). The temporal variation of seismic noise levels (solid line) in 5-15 Hz (2-4 Hz for Beijing and Enshi) is compared with daily confirmed cases (histogram). The seismic noise level decreases after the COVID-19 outbreak. The noise level reduction (ΔL) varies between -96 and -9 %. The number of daily confirmed cases reduces in 11-32 days after the noise-level decrease. The dates of lockdown or equivalent governmental actions (blue arrow) and lockdown release (red arrow) are marked. The first dates of 10, 50, 100 and 500 daily confirmed cases (N_{10} , N_{50} , N_{100} , and N_{500}) are annotated.

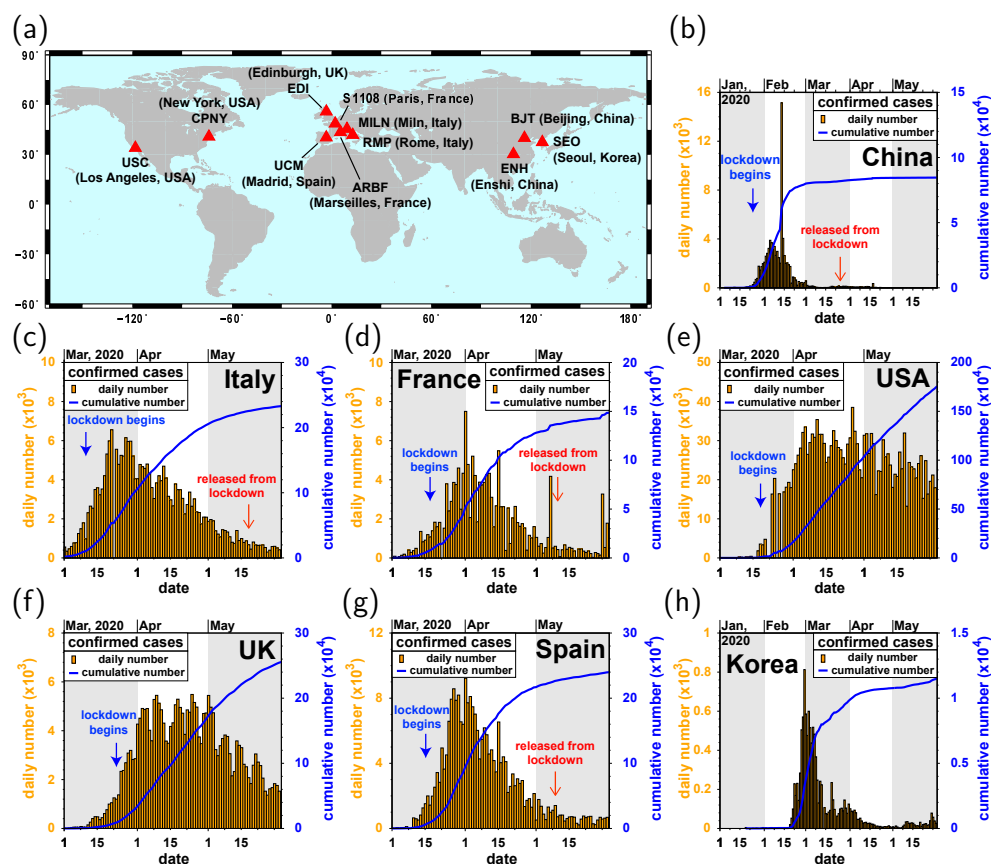


Figure 1. (a) Map of 11 seismic stations in 7 countries and temporal variations of confirmed cases for (b) China, (c) Italy, (d) France, (e) United States of America, (f) United Kingdom, (g) Spain, and (h) South Korea. Continuous vertical seismic records are collected from the seismic stations. The daily and cumulative numbers of confirmed cases are presented. The lockdown starting dates and released dates are marked.

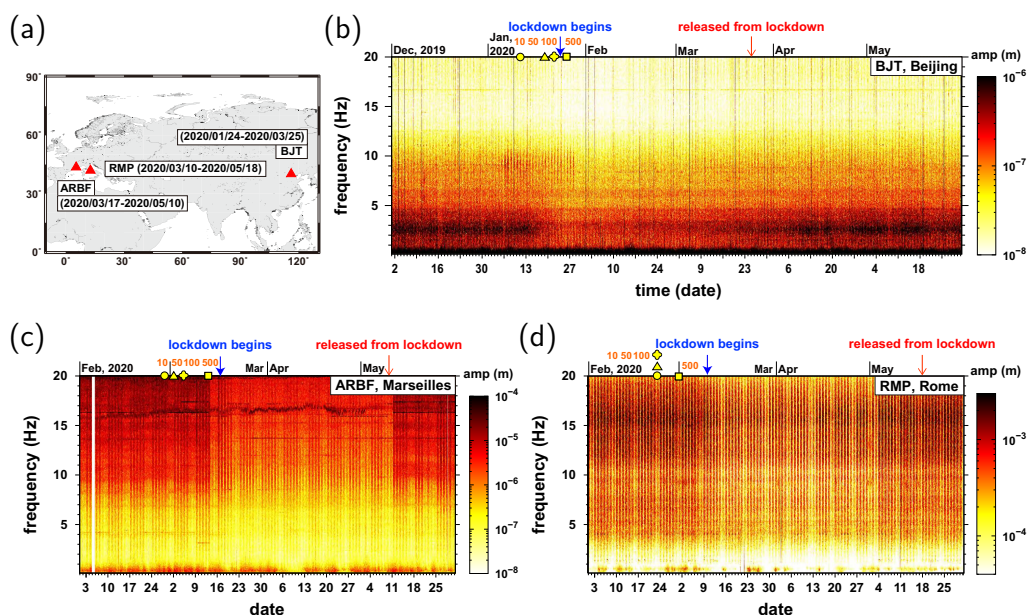


Figure 2. Temporal variation of spectral amplitudes: (a) map of stations and periods, and vertical spectrograms for stations (b) BJT, (c) ARBF, and (d) RMP. The lockdown starting dates and released dates are indicated. The first dates of 10, 50, 100, 500 daily confirmed cases are marked. The seismic noises decrease apparently during the lockdown periods.

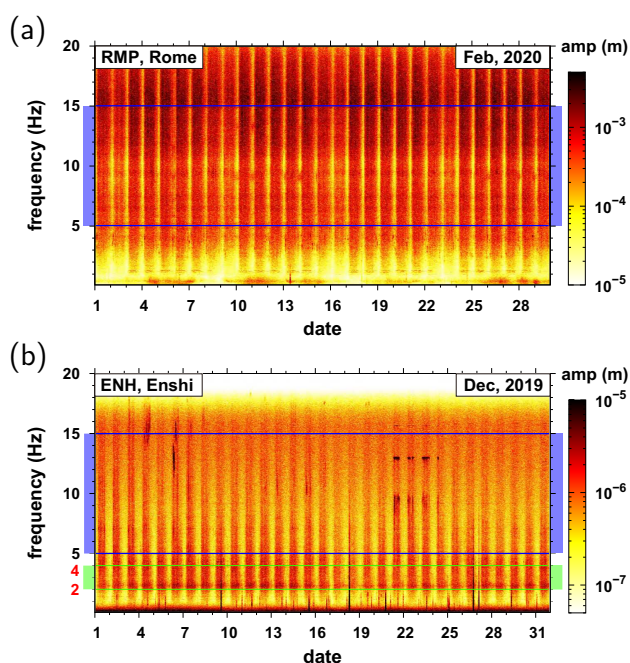


Fig. 3. Spectral contents of ambient seismic noises before the COVID-19 outbreak at stations (a) RMP in Rome and (b) ENH in Enshi. Ambient seismic noises in frequencies ≥ 2 Hz present daily periodicity and diurnal variations associated with human activities. Frequency bands of 5-15 Hz or 2-4 Hz are used for seismic noise analysis.

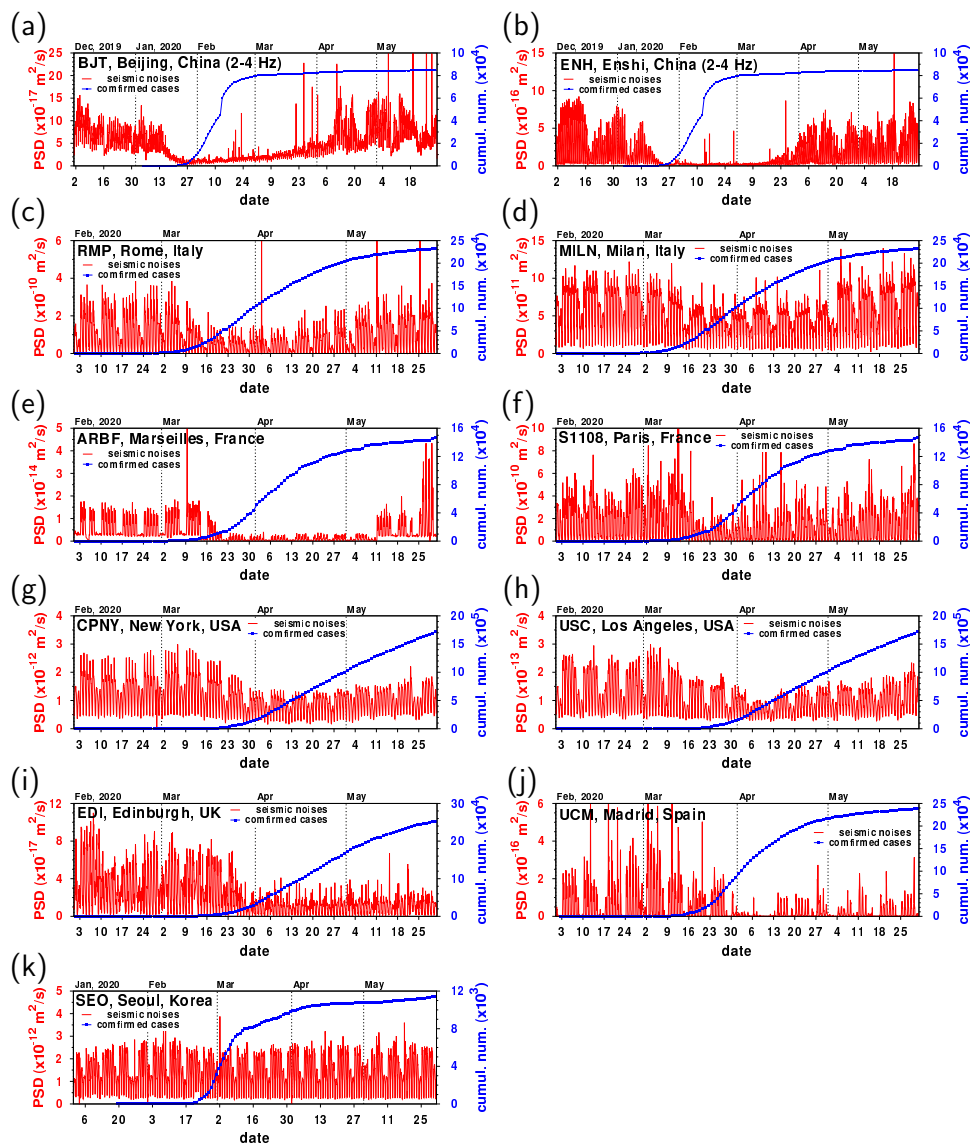


Figure 4. Vertical power spectral density (PSD) variation at frequencies of 5-15 Hz or 2-4 Hz in stations (a) BJT in Beijing, (b) ENH in Enshi, (c) RMP in Rome, (d) MILN in Milan, (e) ARBF in Marseilles, (f) S1108 in Paris, (g) CPNY in New York, (h) USC in Los Angeles, (i) EDI in Edinburgh, (j) UCM in Madrid, and (k) SEO in Seoul. Power spectral densities of seismic noises are presented. The cumulative numbers of confirmed cases are presented. The noise levels are low in March and April in most stations.

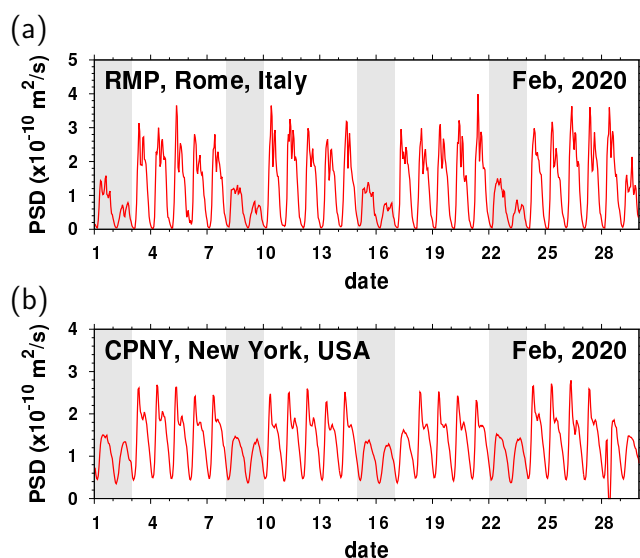


Fig. 5. Vertical power spectral densities in frequencies of 5-15 Hz at stations (a) RMP in Rome and (b) CPNY in New York in February 2020 before the virus outbreak in Italy. Weekends (Saturdays, Sundays) are marked. The seismic-noise amplitudes are large in weekdays, and small in weekends.

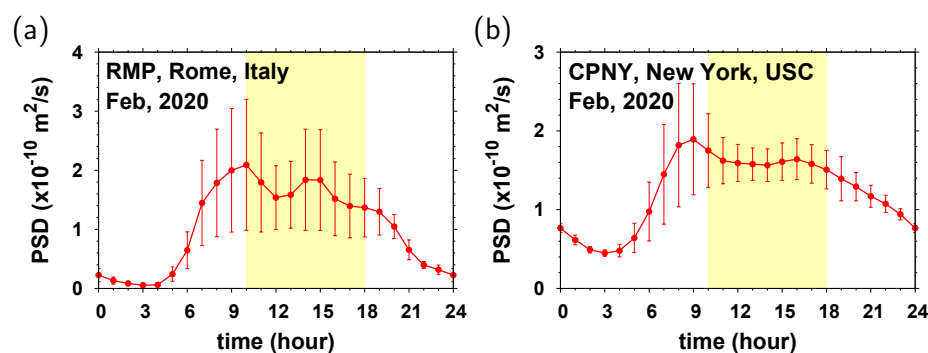


Fig. 6. Diurnal variation of seismic noise amplitudes in weekdays at stations (a) RMP in Rome and (b) CPNY in New York. The analyzed daytime seismic noises are marked. The daytime noise levels are larger than the nighttime noise levels. The seismic noises are weak in lunchtime.

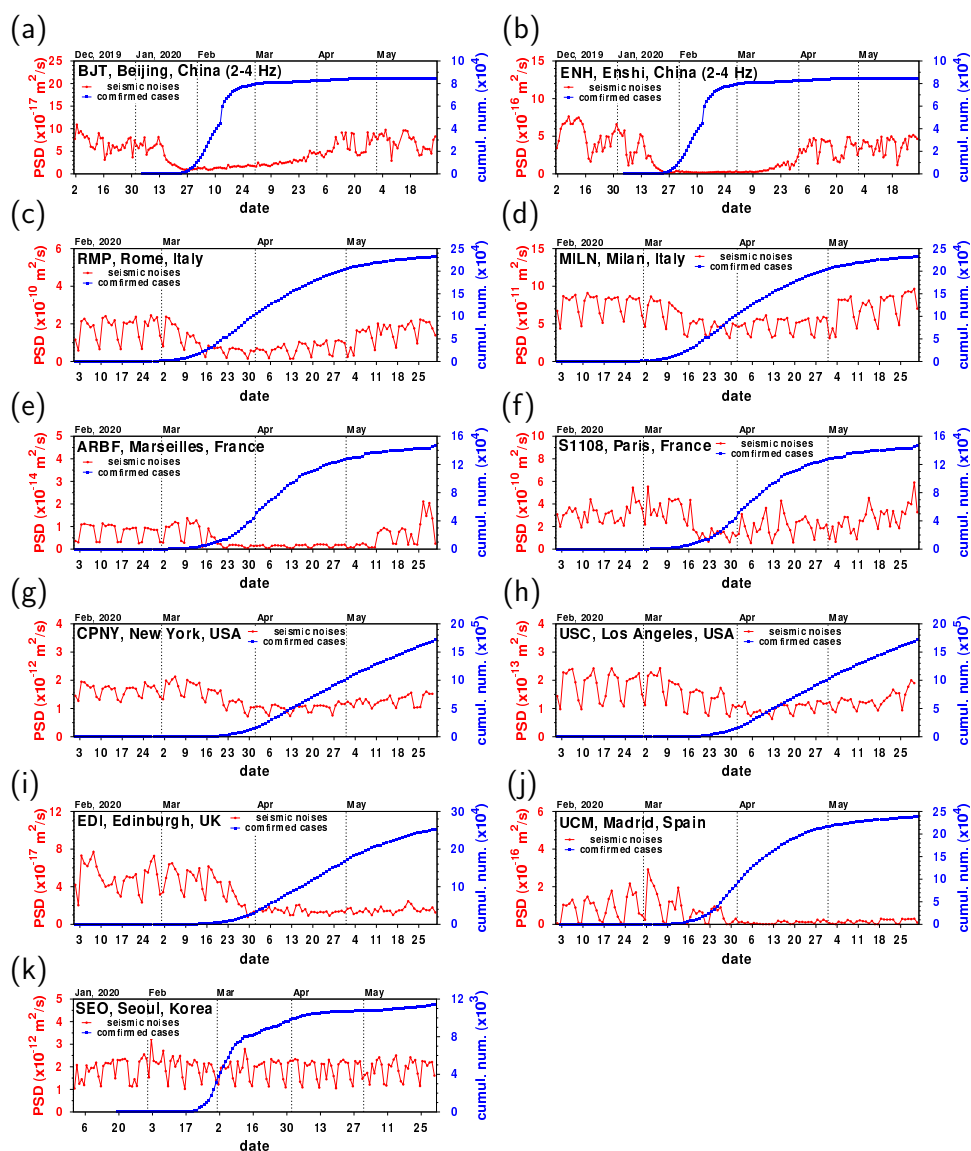


Figure 7. Daily average seismic noise levels at frequencies at frequencies of 5–15 Hz or 2–4 Hz in stations (a) BJT in Beijing, (b) ENH in Enshi, (c) RMP in Rome, (d) MILN in Milan, (e) ARBF in Marseilles, (f) S1108 in Paris, (g) CPNY in New York, (h) USC in Los Angeles, (i) EDI in Edinburgh, (j) UCM in Madrid, and (k) SEO in Seoul. Power spectral densities of seismic noises are presented. The cumulative numbers of confirmed cases are presented.

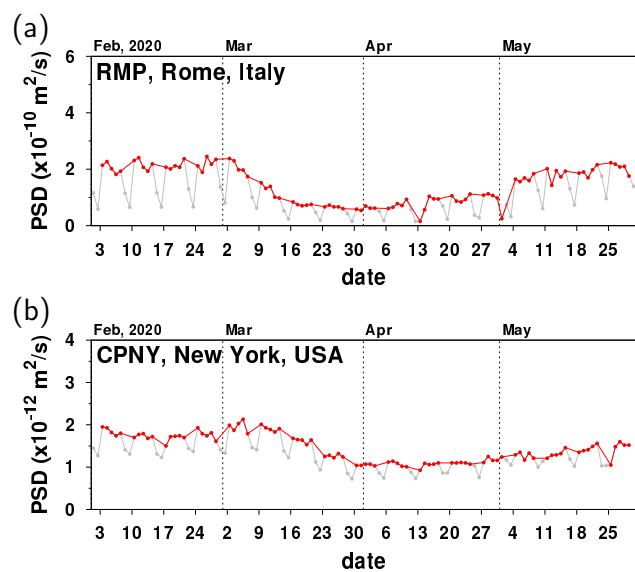


Fig. 8. Representative daily seismic noise variation at stations (a) RMP in Rome and (b) CPNY in New York. The noise levels in weekends are excluded to avoid the weekend effect. The noise levels in weekends are presented for comparison.

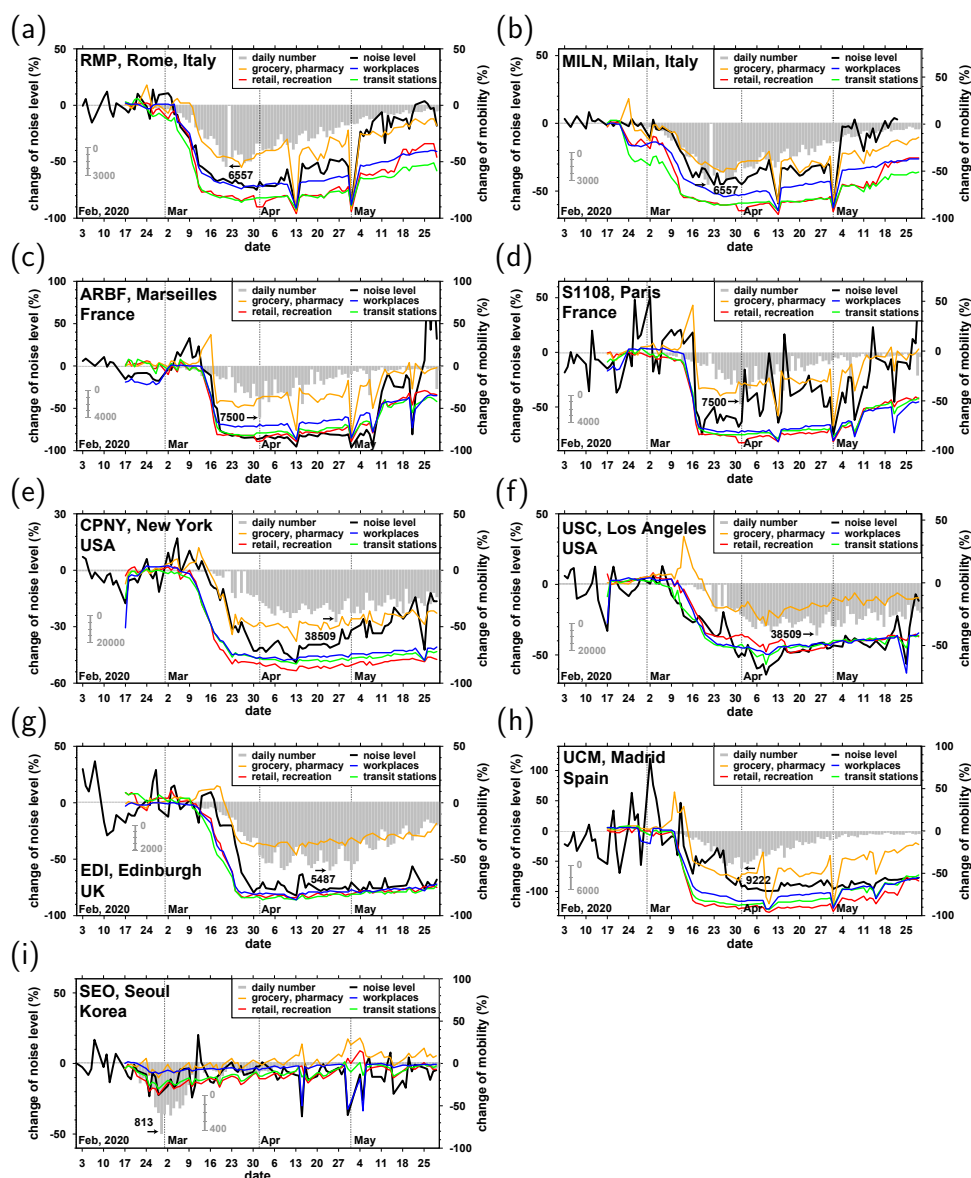


Figure 9. Comparison between seismic noise level changes and mobility data at stations (a) RMP in Rome, (b) MILN in Milan, (c) ARBF in Marseilles, (d) S1108 in Paris, (e) CPNY in New York, (f) USC in Los Angeles, (g) EDI in Edinburgh, (h) UCM, Madrid, and (g) SEO in Seoul. The daily numbers of confirmed cases are presented.

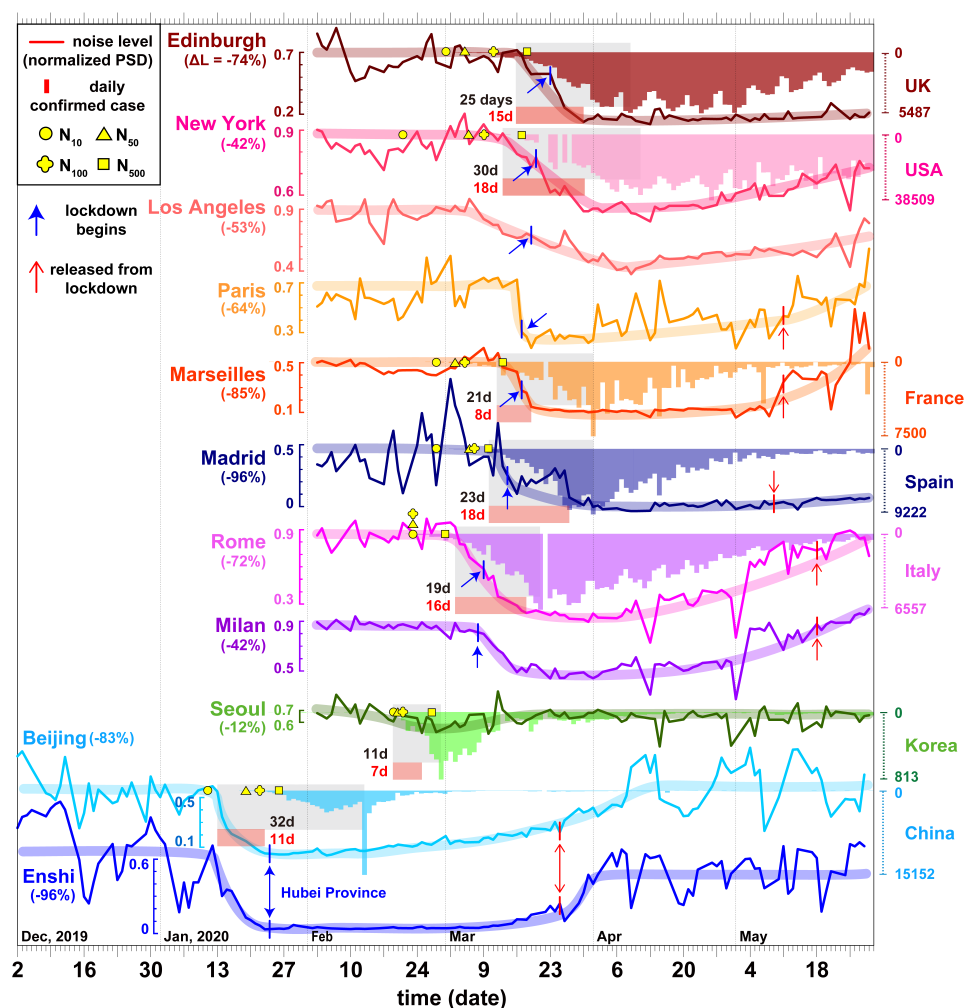


Figure 10. Ambient noise-level changes and daily confirmed cases in 7 countries (UK, USA, France, Spain, Italy, South Korea, and China). The temporal variation of seismic noise levels (solid line) in 5–15 Hz (2–4 Hz for Beijing and Enshi) is compared with daily confirmed cases (histogram). The seismic noise level decreases after the COVID-19 outbreak. The noise level reduction (ΔL) varies between -96 and -9 %. The number of daily confirmed cases reduces in 11–32 days after the noise-level decrease. The dates of lockdown or equivalent governmental actions (blue arrow) and lockdown release (red arrow) are marked. The first dates of 10, 50, 100 and 500 daily confirmed cases (N_{10} , N_{50} , N_{100} , and N_{500}) are annotated.